Pergamon

Cement and Concrete Research 33 (2003) 651–661

CEMENT AND CONCRETE RESEARCH

Physico-chemical study of Cretan ancient mortars

P. Maravelaki-Kalaitzaki[a,*], A. Bakolas[b], A. Moropoulou[b]

[a]25th Department of Prehistoric and Classical Antiquities, Chania, Ministry of Culture, 21 Chalidon Street, Chania, Crete 73100, Greece
[b]Section of Materials and Engineering, National Technical University of Athens, 9 Iroon Polytechniou, Athens 15776, Greece

Received 26 March 2002; accepted 21 October 2002

Abstract

Mortars from monuments of various periods in Crete, from Minoan up to now, have been studied (concerning mineralogical and chemical composition, grain size distribution, raw materials, tensile strength) in order to assess their durability in a marine and humid environment. The lime technology and raw materials, irrespective of the various historic periods, diversify the final composites into mortars, such as: (a) lime, (b) hydraulic lime, (c) lime with crushed brick, and (d) lime with pozzolanic material. These present binders in quantities ranging from 22% (pozzolanic mortars) to 29% (lime mortars). Hydraulic compounds, such as calcium silicate/aluminate hydrates, and tensile strength are higher in the pozzolanic mortars followed by crushed brick lime, hydraulic lime, and lime mortars. High quantities of water-soluble salts identified in the lime mortars indicate their risk of disintegration. A calculation procedure is presented herein, based on the combination of mineralogical and chemical analyses that allows the determination of the binder/aggregate proportion.

Keywords: Ancient mortars; Characterization; Hydraulic lime; Physico-chemical studies; Binder proportion

1. Introduction

The degradation of structural elements (stones and bricks) of historical buildings raises much interest among scientists in both laboratory and in-field studies [1]. However, only limited knowledge is available on the deterioration of mortars, which—being the binders of the ancient masonry—experience the heaviest effects of degradation. Sabbioni et al. [2], in studying the atmospheric deterioration of ancient and modern hydraulic mortars, reveal that gypsum, along with the interaction products of gypsum with the binder constituents, was formed from atmospheric pollution. Even though the decay effects of marine aerosol on stone surfaces have been well investigated [3], little knowledge exists on the corrosion of mortars in coastal areas where the marine aerosol influence is evident. In particular, Perry and Duffy [4], studying the salt-induced decay processes on stone units with mortar joints exposed to rainwash in Dublin, found that mortars act as sinks of environmentally derived ions and as sources of mortar-derived ions in well-washed surface environments.

In the historic monuments of Crete, ancient mortars of great quality and strength were observed, showing complete carbonation and satisfactory performance in the humid and marine environment of the island [5–7]. The new restoration mortars, however—uncritically prepared in mixing the raw materials—fail to ensure a physico-chemical, mechanical, and esthetic compatibility with the old masonry and architectural surfaces. Due to the high content of soluble salts, cement mortars demonstrate a limited compatibility with the original components of the masonry. The inadequacy and the incompatibility of modern restoration mortars to the ancient masonry are mainly due to the nature and production technology of the raw materials (e.g., firing temperature, lime slaking, etc.), as well as to the grain size distribution and binder/aggregate ratio of the mortar.

In this context, the investigation into the traditional production technology of mortars and plasters is of great significance in achieving an effective conservation of mortar. More specifically, the mineralogical and chemical composition, along with the texture, microstructure, and grain size distribution, must be carefully considered in order to under-

* Corresponding author. Tel.: +30-28210-44418; fax: +30-28210-94487.
E-mail addresses: Noni.Maravelaki@keepka.culture.gr, nmaravel@electronics.tuc.gr (P. Maravelaki-Kalaitzaki).

0008-8846/02/$ – see front matter © 2002 Elsevier Science Ltd. All rights reserved.
doi:10.1016/S0008-8846(02)01030-X

stand the procedures to produce the final product and the nature of the adhesion bonds [6].

The present study evaluates the mineralogical, physico-chemical, and mechanical characteristics of Minoan, Roman, Hellenistic, Byzantine, and later mortars from buildings in Crete exposed to a marine and humid environment. This study verifies the use of certain materials (whether such materials were used deliberately), the employed technologies, and the physico-chemical characteristics of mortars under marine influences. A procedure for determining the binder/aggregate proportion, based on a combination of chemical and mineralogical analyses, is also reported.

2. Experimental procedure

Mortar sampling was performed on historic monasteries, churches, fortifications, cisterns, and excavations, examining different mortar technologies and exposure conditions. Twenty-eight samples of historic mortars were selected for this study. Samples were taken from the upper parts of buildings to avoid such phenomena caused by capillary rise. The sampling was obtained by chisel on the external and internal portion of joints to analyze both altered and non-altered materials. All analyses were performed on the internal nonaltered portion of joints. Water-soluble ions were measured in both the external (up to 3 cm of depth) and internal portions of mortars (from 5 to 10 cm of depth) in order to ascertain environmental influences. The total sample data were carried out in a significant quantity in order to avoid errors caused by heterogeneity.

In order to obtain information about single components and their grain size distribution, mortar samples were fractionated and sieved through the ISO 565 series of sieves. This allows a better identification of the different mineralogical phases in fractions and an estimation of the proportions of binder/aggregate within the mortar. The most significant fraction of the grain size distribution, for the aim of this research, is that of <63 μm, consisting mostly of the binder. Sometimes, however, significant quantities of fine grain inert could be detected in this fraction [8,9].

The separated samples in aggregate and binder material were examined by mineralogical and physico-chemical analysis. A significant group of 10 samples underwent mechanical tests and the results were correlated with the results of the other analyses. For the mineralogical and physicochemical analyses, the following instrumental techniques were used.

- Thin sections of mortar samples were examined under a polarizing microscope (Zeiss) for the petrographical and mineralogical characterization of the mortar constituents, as well as for microscopic observations on the different mineral phases in the matrix.
- X-ray diffraction (XRD) analysis (Siemens D-500) of finely pulverized samples was performed in order to identify the mineral crystalline phases of the mortars.
- Thermal analyses [thermogravimetry (TG)/differential thermogravimetry (DTG); Mettler TG 50] were performed in order to determine quantitatively the mortar constituents in the total sample by an appropriate analytical procedure [10]. The experiments were carried out on a temperature range of 30–1000 °C with a heating rate of 10 °C/min in a nitrogen atmosphere.
- Calcimetry (Dietrich–Frühling gas volumetric method) was used to determine CO_2 and to compare it with the results of TG/DTG.
- Infrared spectroscopy [Fourier transform infrared spectroscopy (FT-IR); Biorad FTS 40] was used for gathering qualitative information, from a chemical point of view, on some of the characteristic compounds contained in mortars (calcium and magnesium hydroxides and carbonates, gypsum, etc.) and for determining the presence of salts (nitrates, sulphates, oxalates, etc.) as well as organic compounds.
- Chemical analysis of the principal components was carried out by attack with a sodium carbonate–borax alkaline flux and the subsequent analysis of the elements by traditional chemical methods. No standard chemical analysis is yet available, since in several studies, depending on the nature of mortars, different concentrations of acids have been reported [11–13]. For mortars of carbonate sand, more difficulties are encountered in the binder/aggregate separation and subsequent identification of the hydraulic components of the binder. Therefore, acid dissolutions with different concentrations were carried out in several experiments in the laboratory, taking into consideration the methodology proposed in other studies [12–15].
- The aggregates of the studied mortars were also analyzed to determine the carbonate content using the Dietrich–Frühling gas volumetric method. According to this analysis, mixed aggregates were observed in the various grain size fractions ranging from carbonate to siliceous, differing sometimes not only among the various mortars but even in the same mortar. Therefore, the proposed separation of binder/aggregate with a hot HCl treatment was excluded due to the partially carbonate nature of the aggregates [13]. On the basis of the above-mentioned experiments, a methodology is proposed, having two aims: (1) to increase the solubility of the compounds, and (2) to limit the formation of colloidal silica [12]. These two requirements can be fulfilled by using 2 M HCl (1:5) at room temperature for 3 h. The analysis of calcium and magnesium in the acid-soluble fraction was carried out using a titration with ethylenediaminetetraacetic acid (EDTA), as well as murexide and eriochrome black T (eBT) as indicators. The amounts of Fe_2O_3 and Al_2O_3 in the soluble fraction were determined by titration using barium diphenylaminosulphonate and ditizon as indicators. Sodium and potassium were determined by atomic emission spectrometry (AES; Perkin Elmer 3030). The amounts of soluble SiO_2 were determined using AES. The amount of SO_3 is determined by a gra-

vimetric method. The contents of elements after an alkaline fusion of the samples were determined by traditional chemical methods.

- The ions in the water-soluble fractions of mortars and binders were quantified by conductivity measurements estimating the amount of salts present in the historical mortar. The anions in solution of these stone slices (NO_3^-, SO_4^{2-}, Cl^-) were measured using ion chromatography (IC; Dionex 2010i), equipped with an AS11 separator column; the eluent is 20 mM NaOH. Ca^{2+} was determined by means of atomic absorption spectroscopy (AAS), whereas Na^+ and K^+ were measured by atomic emission spectroscopy (AES) both with a Perkin Elmer 3030 spectrometer.
- The tensile strength (fmt,*k*) of the mortars was measured according to the fragment test method [16], permitting measurement of small fragments of mortar [17]. In particular, small historical mortar fragments (gravel size) were taken from the joints and arranged in a special mould within a strong matrix (an epoxy resin or a much stronger mortar).

3. Results and discussion

3.1. Optical microscopy

Optical microscopy observations performed on the studied specimens showed that all the mortars were comprised mainly of calcite with some accessory minerals such as quartz and plagioclase. The appearance of carbonate compounds and broken shells indicated that these aggregates were prepared by either crushing local calcareous sedimentary stones or using sea sand [5]. In particular, crushed brick lime mortars consist of fine to medium aggregates of quartz, plagioclase, and calcite; the fine-grained to medium-grained aggregates of quartz and plagioclase are embedded in the carbonate matrix. In a large number of mortars, pozzolan tracers such as pyroxenes and feldspathoids were found, suggesting the presence of pozzolanic admixtures [2]. Microscopic observations provide ample evidence of products of boundary reactions in crushed brick lime and pozzolanic mortars. Reaction rims at the pozzolanic materials–lime interface were observed in the form of veins along the matrix, filling the vacancies and discontinuities of the mortar structure [18].

3.2. XRD and FT-IR analyses

Table 1 reports the samples per location, historical periods, and use, as well as the mineral compounds as determined from the XRD patterns. The XRD patterns indicate calcite as the main component of the matrix, with the presence of quartz, plagioclase, feldspars, and muscovite as accessory minerals. The XRD analysis of soluble silicates contained in the binder from a significant number of samples reveals hydraulic compounds such as calcium silicate hydrate [C–S–H (9–454), d=3.19(1), 2.84(1), and 2.74(1) Å; tobermorite (10–373), $Ca_5Si_6O_{16}(OH)_2{\cdot}4H_2O$, d=2.83(1) and 11.31(1) Å] and calcium aluminate hydrate (cubic phase C_3AH_6, d=2.04 Å). Minerals associated with pozzolanic earth, i.e., tracers of natural pozzolan, such as diopside, leucite, and analcite, were identified in the binders [2]. The presence of C–S–H and C_3AH_6 in mortars is attributed to the reaction of lime with SiO_2 and Al_2O_3 in the presence of water; SiO_2 and Al_2O_3 may be contained in the natural pozzolan, in the finely ground bricks and tiles, as well as in the lime used [11].

The XRD and the microscopic identification of hydraulic compounds and pozzolanic additives in the matrix of mortars, supported by historical sources, suggest the use of pozzolanic earth of volcanic provenance for the preparation of mortars in Crete. Portlandite was identified in some cases where specific construction techniques or environmental conditions hinder carbonation. Dolomite and other minerals rich in Mg like chlorite and anthophyllite are present in some mortars from Rethymnon and Heraklion. Salt crystallization is evidenced by the presence of halite in *quasi* all mortars. Furthermore, gypsum and potassium nitrate were also identified in several mortars. Potassium nitrate was evidenced by FT-IR analysis in the water-soluble part of mortars.

3.3. Thermal analysis

Thermal analysis is used as a tool in characterizing the historic mortars of Crete, revealing the production process [10], since this analysis confirms the presence of hydraulic characteristics and easily detects the presence of the main components and the nature of aggregates. Table 2 and Fig. 1 report the results of thermogravimetric analyses for mortars, along with the classification of mortars according to the levels of hydraulicity [10]. In Table 2, the temperature ranges correspond to the weight loss due to adsorbed water (20–120 °C), loss of water of hydrated salts (120–200 °C), loss of chemically bound water (hydraulic water, weight loss percent between 200 and 600 °C) when there are no other compounds that undergo weight loss in this temperature range, and loss of CO_2 (>600 °C) due to the decomposition of carbonates [19]. Fig. 1 shows the ratio of CO_2/hydraulic water (CO_2/H_2O) in relation to the CO_2 (percent weight loss >600 °C) in mortars (Fig. 1).

The analyzed mortars show carbonate aggregates and lime binders together with some pozzolanic additives contributing to the mortar hydraulic character. In particular, based on the CO_2 being bound to carbonates and the water being bound to hydraulic components (in weight loss percent), four groups of mortars were identified [20]—typical lime, hydraulic lime, crushed brick lime, and pozzolanic mortars (Table 2 and Fig. 1):

(a) The typical lime mortars correspond to less than 1.5% water chemically bound to hydraulic components and to CO_2 values between 30% and 38%.

Table 1
Sampling and results of the XRD analyses of the Cretan ancient mortars

Sample, location, and construction period	Composition
Chania, Santa Maria della Misericordia, Venetian period	
SM1 joint mortar, northern wall	Calcite, quartz, halite, muscovite
SM2 joint mortar, southern wall	Calcite, quartz, halite
SM7 joint mortar, eastern inner wall	Calcite, quartz, halite, gypsum, calcium silicate hydrate
Chania, Dockyards, Venetian period	
Na1 joint mortar, northern wall, 17th Dockyard	Calcite, quartz, halite
Na2 joint mortar, eastern outer wall, 17th Dockyard	Calcite, quartz, halite
Nb1 lining mortar, western outer wall, 16th Dockyard	Calcite, quartz, plagioclase, halite, calcium silicate hydrate, tobermorite
Nb2 joint mortar, western outer wall, 16th Dockyard	Calcite, quartz, halite
Chania, Venetian Port, Venetian period with Turkish repairing	
L1 joint mortar, external arm of port, Turkish restoration	Calcite, quartz, halite, gypsum
L3 joint mortar, external arm of port	Calcite, quartz, halite, gypsum, calcium silicate hydrate, muscovite
Chania, Firkas Fortress, Venetian period with Turkish repairing	
F1 joint mortar, southern side of Fortress	Calcite, quartz, halite, plagioclase, chlorite, montmorillonite
F2 joint mortar, northern side of Fortress	Calcite, quartz, halite, calcium silicate hydrate, tobermorite, muscovite
CI1 lining mortar, Chania, Venetian cistern, internal part	Calcite, quartz, plagioclase, sanidine, halite, calcium silicate hydrate
SF1 joint mortar, Loutro, Chania, Roman ruins, northern wall	Calcite, quartz, halite, calcium silicate hydrate
Paleokastron, Heraklion, Venetian fortification with Turkish repairing	
HP1 joint mortar, northern side	Calcite, quartz, plagioclase, halite, illite, calcium silicate hydrate
HP2 joint mortar, eastern side	Calcite, quartz, plagioclase, halite, calcium silicate hydrate
HP3 joint mortar, southern–western side	Calcite, quartz, halite, dolomite, calcium silicate hydrate, chlorite, augite, leucite
HP4 joint mortar, northern side	Calcite, quartz, halite, dolomite, calcium silicate hydrate, plagioclase, diopside
HP5 lining mortar, eastern side	Calcite, quartz, halite, dolomite, calcium silicate hydrate, gypsum, analcite, augite
HP6 joint mortar, northern side	Calcite, quartz, halite, dolomite, plagioclase, calcium silicate hydrate, diopside
HP7 joint mortar, eastern side	Calcite, quartz, halite, chlorite, augite, diopside, leucite, analcite
Chania, ancient Kydonia, excavation ruins	
EF1 plaster, later Minoan period	Calcite, quartz, anthophyllite
EF4 plaster, later Minoan period	Calcite, quartz, anthophyllite, illite, gypsum, sanidine, augite, leucite, diopside
EF5 lining mortar, early Hellenistic period	Calcite, quartz, plagioclase, illite, calcium silicate hydrate
EF6 plaster, early Hellenistic period	Calcite, quartz
Rethymnon, Fortress, Venetian period	
Re7 joint mortar, northern wall	Calcite, quartz, chlorite, gypsum, portlandite
Re8 plaster, southern inner wall	Calcite, quartz, calcium aluminate hydrate
Re13 plaster, entrance, left side	Calcite, quartz, plagioclase, muscovite, dolomite, calcium silicate hydrate, gypsum
Re14 joint mortar, entrance, left side	Calcite, quartz, plagioclase, sanidine, dolomite, calcium silicate hydrate, gypsum

Calcite (5-0586), quartz (5-0490), muscovite (6-0263), plagioclase (9-466, 9-465, 9-467), sanidine (19-1227), dolomite (11-78), chlorite (12-242), calcium aluminate hydrate (2-79), calcium silicate hydrate (9-454), gypsum (6-0046), portlandite (4-733), halite (5-628), anthophyllite (9-455), illite (29-1496, 26-0911), tobermorite (10-373), montmorillonite (13-259), augite (24-202), diopside (11-654), leucite (15-47), analcite (19-1180).

Table 2
TG/DTG analysis of the total samples (*M*) and CO_2/H_2O ratio (weight loss percent >600 °C/weight loss percent between 200 and 600 °C)

Samples		Weight loss per temperature range (%)				
		<120 °C (*M*)	120–200 °C (*M*)	200–600 °C (*M*)	>600 °C (*M*)	CO_2/H_2O (*M*)
Typical lime mortars ($n=7$)	Mean	0.6	0.55	1.33	34.58	26.00
	S.D.	0.18	0.10	0.26	3.86	2.98
Hydraulic lime mortars ($n=8$)	Mean	1.19	1.22	5.06	30.65	6.06
	S.D.	0.27	0.69	0.99	3.31	1.81
Crushed brick lime mortars ($n=7$)	Mean	1.40	0.91	4.46	24.94	5.59
	S.D.	0.34	0.25	0.38	1.39	0.26
Pozzolanic mortars ($n=6$)	Mean	2.91	1.50	9.74	18.78	1.93
	S.D.	1.28	0.57	2.10	1.21	0.49

n = the number of the investigated samples for each group.

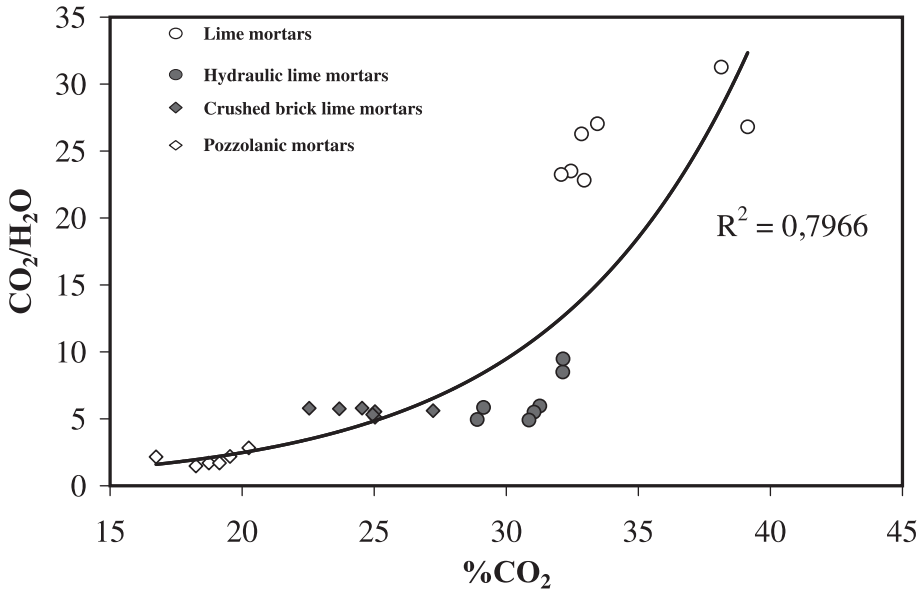

Fig. 1. CO_2/H_2O ratio (weight loss percent >600 °C/weight loss percent between 200 and 600 °C) versus CO_2 percent (weight loss percent >600 °C) referred to the total mortar sample.

(b) The hydraulic lime mortars contain CO_2 ranging between 27% and 34% and chemically bound water up to 5%. This group presents intermediate hydraulic character.
(c) The crushed brick lime mortars show hydraulic water and CO_2 content in the range of 4–5% and 24–26%, respectively. This group presents higher hydraulic character than the hydraulic lime mortars.
(d) The pozzolanic mortars, showing more than 7% hydraulic water content and less than 20% CO_2, present the more advanced hydraulic character.

The inverse trend of hydraulicity (CO_2/H_2O) of the mortar samples is shown to augment exponentially with CO_2. The pozzolanic and crushed brick mortars are con-

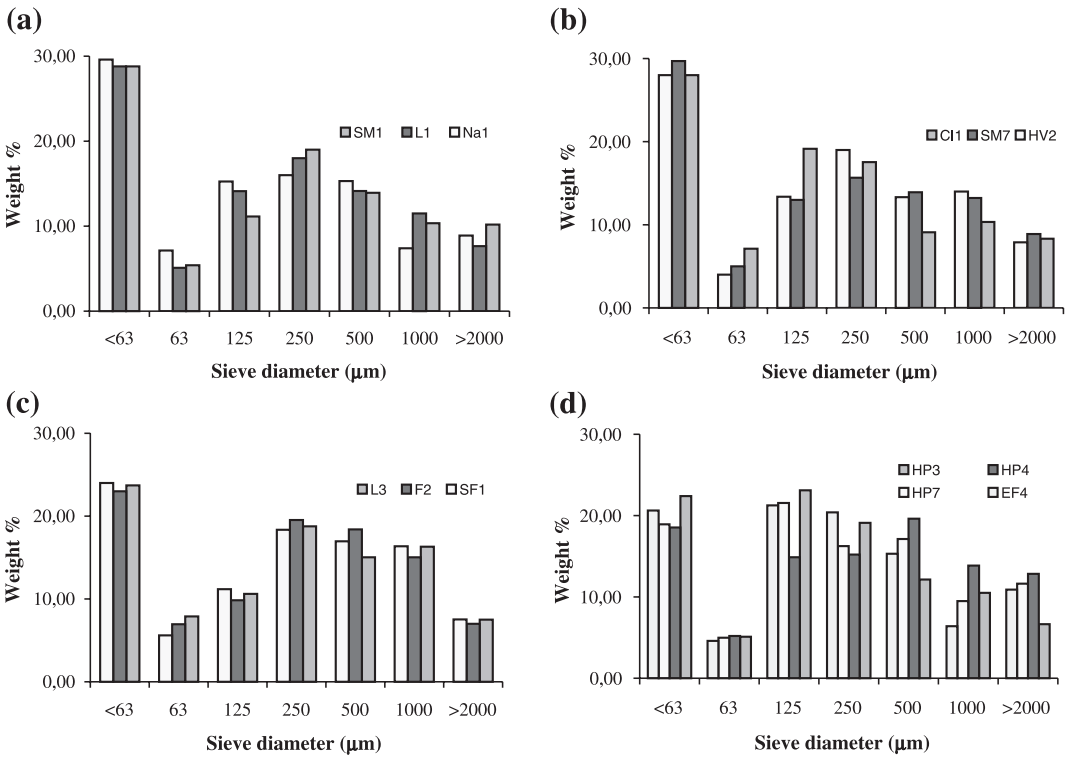

Fig. 2. Grain size distribution of (a) lime mortars, (b) hydraulic lime mortars, (c) crushed brick lime mortars, and (d) pozzolanic mortars.

centrated at the bottom of Fig. 1, the hydraulic lime in the middle of the curve, and the typical lime at the upper right in ratios of CO_2/H_2O>20% and CO_2>30%.

3.4. Grain size distribution

The grain size distribution is an important analysis in obtaining information on the single components of mortars and their mixture ratio during mortar preparation [8–10,20]. The grain size distribution of the above-classified mortars and plasters after fractionation and sieving is shown in Fig. 2. Lime mortars present an average of 30% of binding material in the <63 μm range, while 60% of the total material has grain size between 125 and 1000 μm, with a maximum around 250 μm (Fig. 2a). The fine sand fraction (125–500 μm) turns out to be, in percentage terms (50%), the most important fraction. Few fragments have diameters greater than 2000 μm. This grain size distribution permits the estimation of the binder/aggregate ratio per weight of lime mortars from 1/3 to 1/2, irrespective of the various historic periods. Crushed brick and pozzolanic mortars (Fig. 2c and d), compared with typical lime and hydraulic lime mortars (Fig. 2a and b), reveal less binding material. Crushed brick and pozzolanic mortars have the coarser aggregates, while the hydraulic lime mortars have the finest. In the hydraulic lime, crushed brick, and pozzolanic mortars, a binder/aggregate ratio of 1/3 per weight could be selected as the proper mixture ratio for mortars from Classical and Byzantine monuments.

3.5. Chemical analysis

In this study, the complete characterization of representative samples from each group was accomplished. Table 3 includes the results of the complete chemical analysis of four representative samples from the four classes of mortars. In Tables 4 and 5, the results of the chemical analysis of the soluble and insoluble fraction resulting from the acid attack [with 2 M HCl (1:5) at room temperature for 3 h] for the same mortars are reported. In Fig. 3, the values for conductivity in the aqueous extraction and the ion values identified for the internal and external parts of the above-analyzed mortars are shown.

The complete chemical analysis turns out to be a valid reference in comparing the results achieved by other techniques of characterization. Calcium carbonate (calcium oxide and calcination loss) and silica were the main components determined. Silica content (see Table 3) was highest in the pozzolanic and crushed brick lime mortars (33% and 27%, respectively), while the hydraulic and lime mortars show lower values (12% and 6%, respectively). The magnesium content is generally low in all cases except for the pozzolanic mortars, in which the dolomite is responsible for the detected values of MgO. In the other mortars, the detected quantity of MgO is mainly due to the presence of Mg-rich minerals.

The amount of CaO determined by the CO_2 evolution (CaO_{Cc}; Table 3), which corresponds to the calcite content of mortars, is differentiated from the total CaO in all mortars expect the lime ones, indicating that it is bound to other chemical compounds apart from calcite. The molecular excess of the acid soluble CaO ($CaO_{acid\ sol}$) towards the CaO bound to calcite (CaO_{Cc}) expresses the CaO content bound to hydraulic aluminosilicates (CaO_{sil}), which are mostly attributed to the binder (Table 4). For this calculation, in mortars containing gypsum (e.g., L1, SM7, L3, and EF4), the amount of acid-soluble SO_3 was totally attributed to the gypsum quantity; therefore, the corresponding CaO amount was subtracted from the $CaO_{acid\ sol}$. The evidence for the presence of gypsum is its identification with FT-IR, TG/DTG, and XRD analyses, since the acid-soluble SO_3 identified in other samples may be associated with other salts, such as sodium sulphate, ammonium sulphate, etc., which frequently occur in the marine environment. The CaO_{sil}, if correlated both to the high values of silica and the largest amounts of Fe and Al oxides found in pozzolanic mortars compared to the lime ones [e.g., Table 3: $R_2O_3(Fe_2O_3 + Al_2O_3) = 6.8\%$ in pozzolanic mortars, versus 1.3% in lime ones], suggest that hydraulic silicates occur in pozzolanic mortars.

Table 3
Complete chemical analysis of the samples

	%CaO	%MgO	%SiO_2	%R_2O_3	%Na_2O	%K_2O	CaO_{Cc}	%SO_3
Lime mortars								
L1	42.39	0.56	6.64	1.45	1.28	0.91	41.09	8.45
Na1	42.12	0.89	6.35	0.89	1.26	0.95	42.05	9.12
SM1	41.10	1.87	8.11	2.54	1.21	1.31	40.50	6.25
EF6	50.54	0.92	2.88	0.41	0.31	0.29	50.05	2.57
Mean	44.04	1.06	6.00	1.32	1.02	0.87	43.42	6.60
S.D.	4.37	0.56	2.21	0.92	0.47	0.42	4.46	2.95
Hydraulic lime mortars								
CI1	41.53	0.98	12.86	3.11	0.11	0.21	40.12	2.11
SM7	42.52	1.17	10.37	3.85	0.23	0.26	39.26	1.98
HP1	42.02	1.53	10.73	4.23	0.35	0.52	39.58	2.05
HP2	39.67	0.32	15.78	4.12	0.55	0.68	36.96	2.14
Mean	41.44	1.00	12.44	3.83	0.31	0.42	38.98	2.07
S.D.	1.24	0.51	2.49	0.50	0.19	0.22	1.33	0.07
Crushed brick lime mortars								
L3	34.14	1.19	29.69	4.12	0.09	0.31	30.70	1.14
F2	33.12	1.25	28.65	4.14	0.21	0.36	31.85	1.98
SF1	36.38	1.32	21.25	5.34	0.34	0.48	34.27	1.08
EF5	33.48	1.36	27.47	4.25	0.61	0.78	31.15	1.25
Mean	34.28	1.28	26.77	4.46	0.31	0.48	31.99	1.36
S.D.	1.46	0.08	3.79	0.59	0.22	0.21	1.59	0.42
Pozzolanic mortars								
HP3	25.58	3.40	31.89	6.13	0.24	0.31	23.98	0.85
HP4	28.54	2.95	31.24	6.12	0.19	0.32	25.91	0.41
HP7	28.01	1.18	32.45	7.58	0.34	0.87	24.54	1.23
EF4	24.04	1.20	37.14	7.45	0.85	0.78	21.10	1.38
Mean	26.54	2.18	33.18	6.82	0.41	0.57	23.88	0.97
S.D.	2.11	1.16	2.69	0.80	0.30	0.30	2.02	0.43

Sodium carbonate–borax alkaline flux.
Percentages related to original dry mortar.
R_2O_3 expresses the percentages of Fe and Al oxides.
CaO_{Cc} corresponds to CO_2 evolution determined by the gas volumetric method.

Table 4
Chemical analysis of the acid-soluble fraction of the samples

	%CaO	%MgO	%SiO_2	%R_2O_3	%Na_2O	%K_2O	%SO_3	CaO_{sil}
Lime mortars								
L1	42.14	0.51	1.18	0.95	1.11	0.85	4.36	<0
Na1	41.95	0.85	1.12	0.85	1.06	0.76	4.12	<0
SM1	40.78	1.55	1.12	1.13	0.98	0.92	3.16	0.28
EF6	50.41	0.89	0.77	0.37	0.14	0.11	4.83	0.36
Mean	43.82	0.95	1.05	0.83	0.82	0.66	4.12	0.16
S.D.	4.43	0.43	0.19	0.32	0.46	0.37	0.70	0.19
Hydraulic lime mortars								
CI1	40.85	0.89	3.74	1.05	0.05	0.06	0.98	0.73
SM7	42.12	0.93	2.14	1.15	0.10	0.07	1.45	1.85
HP1	42.11	1.11	3.78	1.57	0.25	0.09	1.36	2.53
HP2	39.24	0.23	2.12	1.26	0.45	0.13	0.86	2.28
Mean	41.08	0.79	2.95	1.26	0.21	0.09	1.16	1.85
S.D.	1.36	0.39	0.94	0.23	0.18	0.03	0.29	0.80
Crushed brick lime mortars								
L3	34.05	0.99	2.11	2.11	0.03	0.05	0.85	2.76
F2	32.87	1.14	2.34	2.85	0.11	0.03	0.63	1.02
SF1	36.11	1.11	5.02	2.96	0.09	0.05	1.25	1.84
EF5	33.41	1.23	2.99	2.16	0.21	0.09	1.36	2.26
Mean	34.11	1.12	3.12	2.52	0.11	0.06	1.02	1.97
S.D.	1.42	0.10	1.32	0.45	0.07	0.03	0.34	0.73
Pozzolanic mortars								
HP3	24.87	2.82	6.36	3.20	0.11	0.08	1.56	0.89
HP4	27.23	1.75	5.38	3.89	0.09	0.02	1.07	1.32
HP7	27.56	1.14	4.87	4.14	0.12	0.07	0.98	3.02
EF4	24.54	1.05	4.89	4.25	0.25	0.11	0.99	2.75
Mean	26.05	1.69	5.38	3.87	0.14	0.07	1.15	1.99
S.D.	1.56	0.81	0.70	0.47	0.07	0.04	0.28	1.05

Percentages related to original dry mortar.
R_2O_3 expresses the percentages of Fe and Al oxides.
CaO_{sil} expresses the CaO content bound to hydraulic calcium silicates ($CaO_{sil} = CaO_{acid\ sol} - CaO_{Cc} - CaO_{Gy}$).

The soluble silica detected in the acid-soluble fraction of mortars, along with the considerable amounts of R_2O_3 detected in pozzolanic and crushed brick lime mortars (Table 4), established the hydraulic effect of mortars, since they are the most important parameters directly related to the hydraulic effect. Na and K were identified both in the acid-soluble and insoluble fraction, since these elements have also been included as cations within the lattices of nonhydraulic silicates and clays, as well as in the water-soluble salts.

The analysis of the insoluble residue (Table 5) aims at the characterization of the aggregate fraction and obtains information during the XRD analysis for components of low quantity not otherwise directly detectable. It can be seen that the major component in all mortars is SiO_2 (ranging from 28% in pozzolanic mortars to 5% in lime mortars). The aggregate used in lime mortars is fundamentally calcareous, while in other mortars, a siliceous character is also encountered. This silica originates from α-quartz, nonhydraulic silicates, and clays. The nonhydraulic silicates and clays are responsible for the detected Fe_2O_3 and Al_2O_3 contents.

Soluble salts, such as sulphates, chlorides, and nitrates, are evidenced in all types of mortars (Fig. 3). The external part of mortars was mostly affected by crystallization. Mortars possessing high values of total conductivity show a bad state of conservation and have a higher risk of disintegration. In the Fig. 3, it can be seen that conductivity mainly varies with the amounts of sulphates, nitrates, and calcium. It is important to emphasize that lime mortars show higher values of total conductivity than the other mortars even at a depth of 10 cm from the surface (internal portion) and, therefore, are more susceptible to deterioration. The high amounts of soluble salts detected in lime mortars were mainly associated with secondary reactions induced between the calcite of binder and marine salts.

3.6. Determination of the binder/mortar ratio

In the study of mortars, an important drawback has arisen in the determination of the weight of the binder, since, in several cases, the grain size analysis cannot be considered reliable enough for the separation binder/aggregates. This operation is hardly influenced by the operator due to the presence of friable aggregates, such as ceramics, porous stones, etc. In this study, an attempt was made to determine the binder/mortar proportion using the results of the above chemical

Table 5
Chemical analysis of the insoluble residue obtained after hydrochloric attack

	%MgO	%SiO_2	%R_2O_3	%Na_2O	%K_2O	%SO_3
Lime mortars						
L1	0.17	4.99	0.58	0.11	0.07	1.92
Na1	0.22	4.16	0.39	0.08	0.03	1.24
SM1	0.18	4.89	0.93	0.06	0.04	1.39
EF6	0.12	0.58	0.14	0.04	0.08	1.01
Average	0.17	3.66	0.51	0.07	0.06	1.39
S.D.	0.04	2.08	0.33	0.03	0.02	0.39
Hydraulic lime mortars						
CI1	0.13	9.78	1.79	0.04	0.04	0.98
SM7	0.26	7.69	2.14	0.07	0.05	1.11
HP1	0.52	7.22	3.19	0.35	0.06	0.45
HP2	0.24	12.34	3.01	0.43	0.09	1.36
Average	0.29	9.26	2.53	0.22	0.06	0.98
S.D.	0.17	2.34	0.68	0.20	0.02	0.38
Crushed brick lime mortars						
L3	0.14	27.12	2.76	0.02	0.04	0.23
F2	0.58	26.74	2.86	0.08	0.02	0.45
SF1	0.83	16.25	2.85	0.06	0.04	0.11
EF5	0.21	24.03	2.72	0.15	0.06	0.36
Average	0.44	23.54	2.80	0.08	0.04	0.29
S.D.	0.32	5.05	0.07	0.05	0.02	0.15
Pozzolanic mortars						
HP3	2.40	24.98	2.53	0.08	0.06	0.58
HP4	2.38	25.21	3.42	0.06	0.01	0.59
HP7	1.12	26.89	3.91	0.08	0.05	0.41
EF4	0.98	30.12	3.49	0.18	0.08	0.12
Average	1.72	26.80	3.34	0.10	0.05	0.43
S.D.	0.78	2.37	0.58	0.05	0.03	0.22

Percentages related to original dry mortar.
R_2O_3 expresses the percentages of Fe and Al oxides.

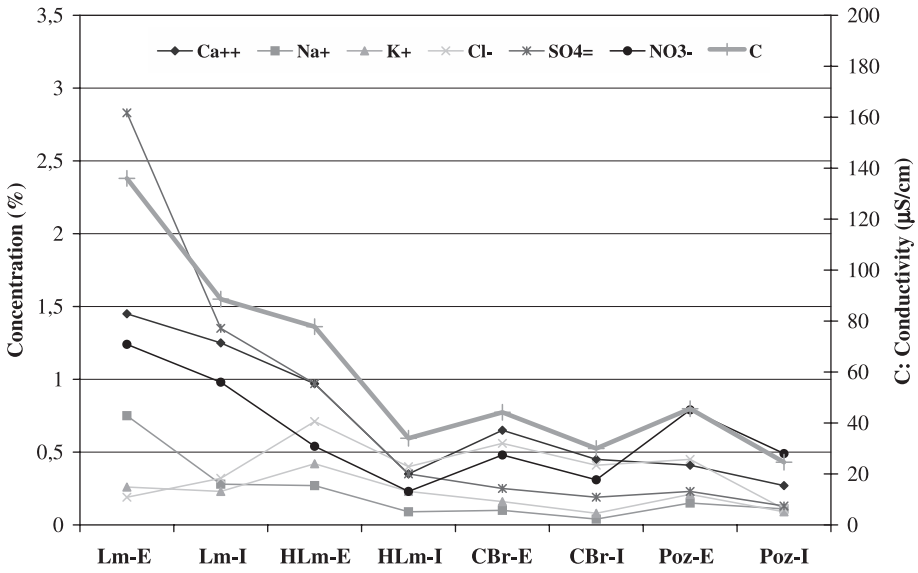

Fig. 3. Results of conductivity (C) and ions concentrations in the aqueous extracts of the external portion (E: up to 3 cm of depth from the surface) and the internal portion (I: from 5 to 10 cm of depth from the surface) for the total mortar samples. Lm, lime mortars; HLm, hydraulic lime mortars; CBr, crushed brick lime mortars; Poz, pozzolanic mortars. (Conductivity, expressed in µS/cm, is given for a suspension of 1 mg/ml sample; the concentrations of ions are expressed as percentages of the samples).

analyses. In order to obtain the aggregate/binder proportion, the results of the complete chemical analysis of the mortars were combined with the results of the acid hydrochloric soluble/insoluble fraction and the mineralogical data, as follows.

The mass of mortar includes the calcite both from binder and aggregates, the chemically bound water determined in the temperature range from 200 to 600 °C, the total soluble salts, and the total Si, Fe, Al, and Mg oxides calculated in the complete chemical analysis of samples (Table 3). In the mortar bulk sample, the quantities of Na_2O, K_2O, and SO_3 determined in the acid-insoluble residue (Table 5) were also included since these mainly originate from the aggregate fraction of mortars. Therefore, the chemical composition of a mortar (C_M) can be described by the following system of equations:

$$C_M = Cc_M + (H_2O_{cb})_M + SS_M + [(MgO) + (SiO_2) + (R_2O_3)]_M + [(Na_2O) + (K_2O) + (SO_3)]_{IR} \quad (1)$$

$$P = Cc_M + (H_2O_{cb})_M + SS_M \quad (2)$$

$$Q = [(MgO) + (SiO_2) + (R_2O_3)]_M + [(Na_2O) + (K_2O) + (SO_3)]_{IR} \quad (3)$$

$$C_M = P + Q \quad (4)$$

where:

- Cc_M is the calcite of mortar;
- $(H_2O_{cb})_M$ is the chemically bound water determined in the thermogravimetric analysis of mortars between 200 and 600 °C;
- SS_M is the quantity of soluble salts determined in the total mass of mortars;
- $[(MgO)+(SiO_2)+(R_2O_3)]_M$ are the oxide determined in the complete chemical analysis of samples (Table 3);
- $[(Na_2O)+(K_2O)+(SO_3)]_{IR}$ is the quantity of Na_2O, K_2O, and SO_3 determined in the acid-insoluble residue (Table 5).

The mass of binder (C_B) includes calcite, soluble salts, the chemically bound water (determined in the range from 200 to 600 °C), and the hydraulic silicates. The latter were calculated by adding to the acid-soluble Si, Fe, and Al oxides the quantity of CaO_{sil}. The chemical composition of the binder can be described by the following system of equations:

$$C_B = Cc_B + (H_2O_{cb})_B + SS_B + CaO_{sil} + [(SiO_2) + (R_2O_3)]_{acid\ sol} \quad (5)$$

$$CaO_{sil} = CaO_{acid\ sol} - CaO_{Cc} - CaO_{Gy} \quad (6)$$

$$R = [(SiO_2) + (R_2O_3)]_{acid\ sol} + CaO_{sil} \quad (7)$$

where:

- Cc_B is the calcite of binder;
- $(H_2O_{cb})_B$ is the chemically bound water of binders;
- SS_B is the quantity of soluble salts of binders;
- $[(SiO_2)+(R_2O_3)]_{acid\ sol}$ are the oxide determined in the acid-soluble fraction of mortars reported in Table 4;
- $(CaO)_{sil}$ is the quantity of CaO bound to silicates (Table 4) by considering the quantities of CaO bound to calcite (CaO_{Cc}) and to gypsum (CaO_{Gy}).

Eqs. (5)–(7) can be described as:

$$C_B = Cc_B + (H_2O_{cb})_B + SS_B + R \quad (8)$$

By considering the total mass of mortars equal to $C_M = 100$ and the weight percentage of binder to the mortar equal to $X_B = x/100$, Eq. (8) can be expressed as a function of the calcite, chemically bound water, and soluble salts of the mortar bulk sample, as follows:

$$C_B = X_B{*}[Cc_M + (H_2O_{cb})_M + SS_M] + R \quad (9)$$

Eq. (9) can be expressed as:

$$C_B = X_B{*}P + R \quad (10)$$

By dividing Eqs. (4) and (10) and also by considering that $C_M = 100$ and $C_B = x$, then the following is obtained:

$$X_B = (X_B{*}P + R)/(P + Q) \quad (11)$$

Therefore, by solving Eq. (11), X_B can be expressed as a function of the identified constituents of mortar bulk sample, as follows:

$$X_B = R/Q \quad (12)$$

In considering the results of the complete chemical analysis of the samples, as well as the chemical analysis of their acid-soluble/insoluble fraction, information on the weight factor of the binder in relation to the total mortar can be obtained. The ratio of SiO_2, R_2O_3, and CaO_{sil} (which are detected in the acid-soluble fraction) to SiO_2, R_2O_3, and MgO detected in the total mortar—along with the Na_2O, K_2O, and SO_3 quantity detected in the acid-insoluble residue—corresponds to the effective proportion of binder to the total mortar. Table 6 shows the binder/mortar proportion. This is derived from chemical analysis through the proposed Eq. (12) compared with the finer grain size fraction (<63 μm) calculated through the grain size distribution. It becomes evident that this consideration applies well to hydraulic mortars but excludes the pure lime mortars, in which generally the major part of the binder consists of calcite without the presence of hydraulic components.

3.7. Mechanical properties

The tensile strength measurements are presented in Table 7. Following the classification deriving from the results of thermal analysis, one may observe a sequence of fmt,k values like: (a) for lime mortars, 0.35>fmt,k; (b) for hydraulic lime mortars, 0.55>fmt,k>0.35; (c) for crushed brick lime mortars, fmt,k>0.55; and (d) for pozzolanic mortars, fmt,k>0.60.

There is an inverse proportionality between the fmt,k measured values and the estimated CO_2/H_2O ratio. Mortars with low values of CO_2/H_2O, as the pozzolanic and crushed brick lime mortars, show high values of the fmt,k, whereas mortars with high values of this ratio (pure lime mortars) correspond to low values of the fmt,k and mortars with intermediate values of the ratio correspond to intermediate values of the fmt,k. Assuming that the binder/aggregate ratio is more or less the same for all mortars under investigation and that aggregates of a calcareous nature prevail, due to which the CO_2/H_2O attains its maximum, one may deduce that the measured tensile strength of the mortars is directly proportional to their level of hydraulicity [20].

Table 6
Binder/mortar proportion (X_B) resulting from the proposed procedure and the correlation to the results of the grain size distribution (Y_B)

	Q	R	$X_B = R/Q$	Y_B
Lime mortars				
L1	10.75	2.13	0.20	0.29
Na1	9.48	1.97	0.21	0.30
SM1	14.01	2.53	0.18	0.29
Mean	11.41	2.21	0.20	0.29
S.D.	2.34	0.29	0.01	0.01
Hydraulic lime mortars				
CI1	18.01	5.52	0.31	0.28
SM7	16.62	5.14	0.31	0.30
HP2	22.11	5.66	0.26	0.28
Mean	18.91	5.44	0.29	0.29
S.D.	2.85	0.27	0.03	0.01
Crushed brick lime mortars				
L3	35.29	6.98	0.20	0.25
F2	34.59	6.21	0.18	0.24
SF1	28.12	9.82	0.35	0.24
Mean	32.67	7.67	0.24	0.24
S.D.	3.95	1.90	0.09	0.00
Pozzolanic mortars				
HP3	42.14	10.45	0.25	0.26
HP4	40.97	10.59	0.26	0.20
HP7	41.75	12.03	0.29	0.20
EF4	46.17	11.89	0.26	0.20
Mean	42.76	11.24	0.26	0.22
S.D.	2.33	0.83	0.02	0.03

Q=[(MgO)+(SiO_2)+(R_2O_3)]$_M$+[(Na_2O)+(K_2O)+(SO_3)]$_{IR}$ (Tables 3 and 5).
R=[(SiO_2)+(R_2O_3)]$_{acid\ sol}$ + CaO_{sil} (Table 4).
Y_B is the binder proportion according to the grain size distribution (finer fraction <63 μm).

3.8. General considerations

From the above analysis of the physico-chemical characteristics of historical mortars, it can be seen that in several cases, mortars with the same ratio and gradation can be characterized by different physico-chemical behaviours. This is due to the effect of the various technical characteristics of the raw materials used and the procedures employed in mortar production. The physico-chemical characterization of historical mortars permits the identification of types of raw materials and differences in mortar types, as well as indicating traditional mortar practice.

Repair mortars should have characteristics as similar as possible to those of the materials to be repaired. Limitations arise from the actual different production technology of raw materials used for the preparation of restoration mortars, such

Table 7
Tensile strength (fmt,*k*) results

	Tensile strength (fmt,*k*) [MPa]
Lime mortars	
L1	0.24
Na2	0.31
Hydraulic lime mortars	
Re8	0.37
Re13	0.44
Crushed brick lime mortars	
L3	0.58
F1	0.58
F2	0.57
Pozzolanic mortars	
HP3	0.62
HP6	0.66
HP5	0.69

as the firing temperature of bricks, the quality of the lime, etc. Furthermore, the new restoration mortars fail to ensure a compatibility with the old masonry because of the employment of cement and polymer-based compounds. In particular, the wide employment of cement during restoration has created irreversible damage to the historical masonry due to its physico-chemical and mechanical incompatibility with the original structure.

This study defines certain criteria and specifications in order to prepare restoration mortars. These criteria are correlated with the quality of the raw materials available in the area and the mortar resistance to environmental loadings. Based on the traditional mortar production techniques, especially as indicated in the present study, mortars with natural and artificial pozzolanic material can be used for the restoration of historical buildings.

4. Conclusions

The studied mortars are classified (according to the results of thermal analysis and irrespective of the varying historical periods) into: typical lime, hydraulic lime, and lime with artificial and natural pozzolanic material. The examined mortars show binders in quantities ranging from 22% (pozzolanic mortars) to 29% (lime mortars). Most probably, the leaching out of calcite due to weathering accounts for these low quantities of binding material. The measured tensile strength values of the mortars are directly proportional to their level of hydraulicity.

Lime mortars were prepared by crushing local calcareous sedimentary stones or by using sea sand. The binders are finely crystallized calcite, totally carbonated. These mortars present an average of 30% of binding material, with the employment of fine sands. Lime mortars show the lower values of total and soluble silica, Fe and Al oxides, structurally water-bound to hydraulic components and the higher CO_2 values compared with other groups. The CaO content bound to hydraulic calcium silicates (CaO_{sil}) is limited or negligible, producing a limited amount of hydraulic silicates. Furthermore, the high quantities of Ca^{2+}, Cl^-, and SO_4^{2-} identified in the water-soluble fraction of these mortars indicate their high susceptibility to deterioration. This observation, if correlated with the lower values of both tensile strength and hydraulicity levels, indicates that pure lime mortars demonstrate a bad state of conservation and have a higher risk of disintegration.

Mortars with hydraulic properties such as hydraulic lime, crushed brick lime, and mortars with natural pozzolana contain coarse aggregates consisting of calcite, quartz, feldspar, and phyllosilicate minerals. The binding material is lime, both pure and hydraulic. The hydraulic compounds in the pozzolanic mortars arise from the reactions of $Ca(OH)_2$ with artificial pozzolana and natural earth of volcanic provenance (e.g., earth of Santorini). The existence of hydraulic compounds was evidenced by the detection of high values of soluble hydraulic compounds, as well as from the CaO bound to the hydraulic aluminosilicates. These components confer to mortars resistance to salt decay and environmental loadings, as indicated by the low values of soluble salts and their actual tensile strength. The physico-chemical study of the above mortars indicates that restoration practice should be conducted using raw materials and techniques similar to those employed in the preparation of historical mortars, thus avoiding damage to historical masonry by the use of incompatible materials.

This study points out that combining the results of the complete chemical analysis, the chemical analyses of the acid-soluble/insoluble fraction of mortars, and the mineralogical data information on the weight factor of the binder in relation to the total mortar can be achieved for the hydraulic mortars, apart from the lime ones. Therefore, by considering the results of chemical analysis, as proposed above, certain limitations in the identification of the binder quantity arising from the grain size distribution can be overcome in mortars with hydraulic components.

Acknowledgements

P. Maravelaki-Kalaitzaki wishes to thank Prof. Z. Agioutantis of the Technical University of Crete for helpful discussions, as well as Mr. James McGann for many helpful reviews. The authors would also like to express their gratitude to the reviewers for their valuable contribution to the improvement of this study.

References

[1] L. Binda, A. Saisi, C. Tiraboschi, Investigation procedures for the diagnosis of historic masonries, Constr. Build. Mater. 14 (2000) 199-233.

[2] C. Sabbioni, G. Zappia, C. Riontino, M.T. Blanco-Varela, J. Aguilera, F. Puertas, K. Van Balen, E.E. Toumbakari, Atmospheric deterioration of ancient and modern hydraulic mortars, Atmos. Environ. 35 (2001) 539–548.
[3] F. Zezza, F. Macri, Marine aerosol and stone decay, Sci. Total Environ. 167 (1995) 123–144.
[4] S.H. Perry, A.P. Duffy, The short-term effects of mortar joints on salt movement in stone, Atmos. Environ. 31 (9) (1997) 1297–1305.
[5] A. Moropoulou, A. Bakolas, P. Michailidis, M. Chronopoulos, Ch. Spanos, Traditional technologies in Crete providing mortars with effective mechanical properties, in: C.A. Brebbia, B. Leftheris (Eds.), Structural Studies of Historical Buildings IV, vol. 1, Computational Mechanics Publications, Southampton, Boston, 1995, pp. 151–161.
[6] A. Moropoulou, A. Theodoraki, K. Bisbikou, P. Michaelidis, Restoration synthesis of crushed brick mortars simulating Byzantine lime and material technologies in Crete, in: J.R. Druzik, P.B. Vandiver (Eds.), Materials Issues in Art and Archaeology IV, vol. 352, Publ. Materials Research Society, Pittsburgh, 1995, pp. 759–769.
[7] A. Moropoulou, P. Maravelaki-Kalaitzaki, M. Borboudakis, A. Bakolas, P. Michailidis, M. Chronopoulos, Historic mortars technologies in Crete and guidelines for compatible restoration mortars, in: G. Biscontin, A. Moropoulou, M. Erdik, J. Delgado Rodrigues (Eds.), PACT, Revue du groupe europeen d'etudes pour les techniques physiques, chimiches, biologiques et mathematiques appliqués a l'archeologie, Compatible Materials for the Protection of European Cultural Heritage, vol. 55, Technical Chamber of Greece, Athens, 1998, pp. 55–72.
[8] G. Biscontin, A. Bakolas, A. Moropoulou, E. Zendri, Microstructural characterization of the historical mortars in Venice, in: V. Fassina, H. Ott, F. Zezza (Eds.), 3rd International Symposium on the Conservation of Monuments in the Mediterranean Basin, Conference Proceedings, Publ. Sopritendenza ai Beni Artistici e Storici di Venezia, Venice, 1994, pp. 405–410.
[9] G. Biscontin, A. Bakolas, P. Maravelaki, E. Zendri, Microstructural and composition characteristics of historic mortars in Venice, in: M.J. Thiel (Ed.), Conservation of Stone and Other Materials, Conference Proceedings, vol. 1, Rilem-Unesco, Chapman and Hall, Paris, 1993, pp. 178–185.
[10] A. Bakolas, G. Biscontin, A. Moropoulou, E. Zendri, Characterization of structural Byzantine mortars by thermogravimetric analysis, Thermochim. Acta 321 (1998) 151–160.
[11] K. Callebaut, J. Elsen, K. Van Balen, W. Viaene, Nineteenth century hydraulic restoration mortars in the Saint Michael's Church (Leuven, Belgium). Natural hydraulic lime or cement? Cem. Concr. Res. 31 (2001) 397–403.
[12] M. Dupas, L'analyse des mortiers et enduits des peintures murales et des batiments ancient, Proceedings International Conference on Mortars, Cements and Grouts Used in the Conservation of Historic Buildings, ICCROM, Rome, 1981, pp. 285–286.
[13] J.I. Alvarez, A. Martin, P.J. Garcia Casado, I. Navarro, A. Zornoza, Methodology and validation of a hot hydrochloric acid attack for the characterization of ancient mortars, Cem. Concr. Res. 29 (1999) 1061–1065.
[14] J.I. Alvarez, I. Navarro, A. Martin, P.J. Garcia Casado, A study of the ancient mortars in the north tower of Pamplona's San Cernin church, Cem. Concr. Res. 30 (2000) 1413–1419.
[15] A. Charola, M. Dupas, R. Sheryll, G. Freud, Characterization of ancient mortars: Chemical and instrumental methods, in: P. Parrini (Ed.), Symposium on Scientific Methodologies Applied to Works of Art, Conference Proceedings, Montedison, Progetto Cultura, Florence, 1984, pp. 28–33.
[16] E.S. Katsagarakis, A new tensile test for concrete, Mater. Struct. 20 (120) (1978).
[17] Th. Tassios, C. Vachliotis, C. Spanos, In situ strength measurements of masonry mortars, Proceedings International Conference on Repair and Strengthening of Stone Masonries, ICCROM, Athens, 1989, pp. 53–61.
[18] A. Bakolas, R. Bertoncello, G. Biscontin, A. Moropoulou, E. Tondello, E. Zendri, Chemico-physical interactions among the constituents of historical walls in Venice, in: J.R. Druzik, P.B. Vandiver (Eds.), Materials Issues in Art and Archaeology IV, vol. 352, Publ. Materials Research Society, Pittsburgh, 1995, pp. 771–777.
[19] A. Moropoulou, A. Bakolas, K. Bisbikou, Characterization of ancient, Byzantine and later historic mortars by thermal analysis and X-ray diffraction techniques, Thermochim. Acta 269/270 (1995) 779–795.
[20] A. Moropoulou, G. Biscontin, A. Bakolas, P. Michailidis, J. Basiotis, Historic mortars in Mediterranean Monuments, in: A. Moropoulou, F. Zezza, E. Kollias, I. Papachristodoulou (Eds.), 4th International Symposium on the Conservation of Monuments in the Mediterranean Basin, Conference Proceedings, vol. 3, Publ. Technical Chamber of Greece, Athens, 1997, pp. 213–237.